Molecular elimination in photolysis of fluorobenzene at 193 nm: Internal energy of HF determined with time-resolved Fourier-transform spectroscopy

Chia-Yan Wu, Yu-Jong Wu, and Yuan-Pern Lee

Citation: The Journal of Chemical Physics **121**, 8792 (2004); doi: 10.1063/1.1802537
View online: http://dx.doi.org/10.1063/1.1802537
View Table of Contents: http://scitation.aip.org/content/aip/journal/jcp/121/18?ver=pdfcov
Published by the AIP Publishing

Molecular elimination in photolysis of fluorobenzene at 193 nm: Internal energy of HF determined with time-resolved Fourier-transform spectroscopy

Chia-Yan Wu and Yu-Jong Wu
Department of Chemistry, National Tsing Hua University, Hsinchu 30013, Taiwan

Yuan-Pern Lee[a)]
Department of Chemistry, National Tsing Hua University, Hsinchu 30013, Taiwan and Institute of Atomic and Molecular Sciences, Academia Sinica, Taipei, Taiwan

(Received 1 June 2004; accepted 11 August 2004)

Following photodissociation of fluorobenzene (C_6H_5F) at 193 nm, rotationally resolved emission spectra of HF($1 \leqslant v \leqslant 4$) in the spectral region 2800–4000 cm^{-1} are detected with a step-scan Fourier-transform spectrometer. In the period 0.1–1.1 μs after photolysis, HF($v \leqslant 4$) shows similar Boltzmann-type rotational distributions corresponding to a temperature ~1830 K; a short extrapolation from data in the period 0.1–4.1 μs leads to a nascent rotational temperature of 1920 ± 140 K with an average rotational energy of 15 ± 3 kJ mol^{-1}. The observed vibrational distribution of $(v=1):(v=2):(v=3):(v=4)=(60 \pm 7):(24 \pm 3):(10.5 \pm 1.2):(5.3 \pm 0.5)$ corresponds to a vibrational temperature of 6400 ± 180 K. An average vibrational energy of $33 \pm 9/3$ kJ mol^{-1} is derived based on the observed population of HF($1 \leqslant v \leqslant 4$) and an estimate of the population of HF($v=0$) by extrapolation. The observed internal energy distribution of HF is consistent with that expected for the four-center (α,β) elimination channel. A modified impulse model taking into account geometries and displacement vectors of transition states during bond breaking predicts satisfactorily the rotational excitation of HF. We also compare internal energies of HF observed in this work with those from photolysis of vinyl fluoride (CH_2CHF) and 2-chloro-1,1-difluoroethene (CF_2CHCl) at 193 nm. © *2004 American Institute of Physics.*
[DOI: 10.1063/1.1802537]

I. INTRODUCTION

Competition between three-center and four-center molecular elimination is the subject of extensive study of molecular dynamics because internal distributions of the products are distinct in each process.[1–3] Photolysis of vinyl halides (CH_2CHX, $X=$F, Cl, or Br) at 193 nm is a prototypical system in which both three-center and four-center HX-elimination channels compete. Although experiments of photofragment translational spectroscopy provide detailed mechanisms of various dissociation channels,[4] they provide no information to distinguish between these two molecular elimination channels for production of HX. Step-scan time-resolved Fourier-transform spectroscopy (TR-FTS) has been demonstrated to be more powerful than other techniques such as resonance-enhanced multiphoton ionization (REMPI) or laser-induced fluorescence in determining the internal-energy distributions of reaction products.[2–7] With TR-FTS, we observed rotationally resolved emission of HX from photodissociation of vinyl halides at 193 nm; highly vibrationally and rotationally excited HX are attributed to production via three-center (α,α) and four-center (α,β) elimination channels.[2,3] Extending the investigation to photolysis of 2-chloro-1, 1-difluoroethene (CF_2CHCl) at 193 nm, we observed emission of HCl($v \leqslant 3$) and HF($v \leqslant 4$) both with Boltzmann-type rotational distributions.[5] Energy participation via the four-center elimination channel is nonstatistical; a modified impulse model based on geometries and displacement vectors of transition states during bond breaking predicts satisfactorily the rotational excitation of HX observed in these investigations. A phenyl halide has a structure partially resembling that of a vinyl halide, hence it is of interest to investigate its molecular dissociation channels and to test the model for dissociation dynamics of four-center elimination.

Photodissociation of phenyl halides in the ultraviolet (UV) region is typically less complicated than that of benzene or toluene,[8–10] partly because of the possibility to excite nonbonding electrons of the halogen atom and partly because the bond energy of C–X ($X=$Cl, Br, or I) is smaller than that of the C–H bond on the phenyl ring. Excitation of the nonbonding electron of the halogen atom to an antibonding orbital leads to a prompt direct dissociation along the repulsive surface, whereas excitation of the bonding electron in the phenyl ring leads to an excited state that might dissociate through various direct or indirect processes. Reported investigations on C_6H_5Cl,[11–15] C_6H_5Br,[11,16] and C_6H_5I (Refs. 11 and 17) all show that the major channel in photodissociation at 193 nm is fission of the C–X bond, with both direct and indirect channels being observed.

[a)]Author to whom correspondence should be addressed. Present address: Department of Applied Chemistry, National Chiao Tung University, Hsinchu 30010, Taiwan. Electronic mail: yplee@mail.nctu.edu.tw

In contrast, although the F-elimination channel is energetically accessible at 193 nm (619 kJ mol^{-1}),

$$C_6H_5F + h\nu \rightarrow C_6H_5 + F, \quad \Delta H^\circ = 534 \text{ kJ mol}^{-1}, \qquad (1)$$

Huang *et al.*[18] observed no evidence of this channel. They employed the multimass ion-imaging technique to find that HF-elimination,

$$C_6H_5F + h\nu \rightarrow C_6H_4 + HF, \quad \Delta H^\circ = 283 \text{ kJ mol}^{-1}, \qquad (2)$$

is the major channel and H-elimination,

$$C_6H_5F + h\nu \rightarrow C_6H_4F + H, \quad \Delta H^\circ \cong 467 \text{ kJ mol}^{-1}, \qquad (3)$$

is a minor channel. Observed intensities of fragment ions C_6H_4 and C_6H_4F exhibit a ratio of ~25:1, indicating a branching ratio likely greater than 0.9 for reaction (2). Experimental enthalpies of reaction are derived from enthalpies of formation for C_6H_5F,[19] HF,[20] C_6H_4 (o-benzyne),[21,22] and C_6H_5 (Ref. 23); -115.9 ± 1.3, -273.3 ± 0.7, 440 ± 10, and 339 ± 8 kJ mol^{-1}, respectively. An experimental enthalpy of formation of C_6H_4F is unknown; a value ~352 kJ mol^{-1} is estimated based on theoretical calculations.

We report here investigation of the HF-elimination channel in photolysis of fluorobenzene at 193 nm with time-resolved Fourier-transform spectroscopy and compare the observed internal energy distribution of HF with other similar four-center HF-photoelimination processes.[18]

II. EXPERIMENTS

The apparatus employed to obtain step-scan time-resolved Fourier-transform spectra has been described previously;[5,24,25] only a brief summary is given here. A lens mildly focused the photolysis beam from an ArF laser at 193 nm (Lambda Physik, Optex) to ~3×4 mm^2 at the reaction center with a fluence ~40 mJ cm^{-1}. Filters passing either 2800–4200 cm^{-1} or 3050–5000 cm^{-1} were employed. We used an InSb detector with a rise time of 0.7 μs, and its transient signal was preamplified with a gain factor 10^5 V A^{-1} (EG&G, Judson, PA9-50, 1.5 MHz), followed by amplification by a factor of 100 (Stanford Research Systems, SRS560, 1 MHz) before being digitized with an external data-acquisition board (PAD1232, 12-bit ADC) at 50 ns resolution. Data were typically averaged over 27 laser pulses at each scan step; 2157 scan steps were performed to yield an interferogram resulting in a spectrum of resolution 2.0 cm^{-1}. To improve the ratio of signal to noise (S/N) of the spectrum, 10–30 consecutive time-resolved spectra were subsequently summed to yield a satisfactory spectrum representing emission at intervals 0.5–1.5 μs.

An IR laser beam at 5958 cm^{-1} with a temporal width ~10 ns was directed into the spectrometer and temporal profiles for the amplified signal of the detector were recorded to yield the instrument response function of the detecting system. The IR laser beam was generated from the second Stokes shift of a dye laser (Spectra Physics, PDL-3) at 700.8 nm that was pumped with a Nd-YAG laser (Spectra Physics, Lab170); a single-pass cell filled with H_2 at ~15 bar was employed for Raman shifting. A delay of 1.3 μs was determined for this specific combination of detector, preamplifier, and amplifier.

C_6H_5F was injected into the vacuum chamber as a diffusive beam through a slit-shaped inlet. The vapor pressure of C_6H_5F is ~77 Torr at 298 K and the partial pressure of C_6H_5F in the chamber was ~0.013 Torr. Ar (Scott Specialty Gases, 99.999%) in a minimal amount was added near the entrance port for the photolysis beam to suppress formation of solid deposit on the quartz window. With Ar purging, the pressure of the system was maintained ~35 mTorr. C_6H_5F (Acros, 99%) was used without purification except for degassing; no impurity was detected in its IR spectrum.

III. RESULTS AND ANALYSIS

We irradiated C_6H_5F at 0.26 Torr in a small static multipass cell (~1.5 L, total path length 6.4 m) with an excimer laser at 193 nm (<20 mJ, 20 Hz) for 120 s and recorded conventional infrared absorption spectra with the Fourier-transform spectrometer operating in a continuously scanning mode. The loss of C_6H_5F and formation of acetylene (C_2H_2, 3282 cm^{-1}) and 1,3-butadiyne (C_4H_2, 3329 cm^{-1}) were readily identifiable, whereas absorption of HF and o-benzyne (C_6H_4) was absent.

Experiments on dynamics were performed with the Fourier-transform spectrometer operating in a step-scan mode. To maintain a nearly collisionless condition within 1.0 μs period, the partial pressures of C_6H_5F (0.013 Torr) and Ar (0.022 Torr) were reduced as much as possible while maintaining a satisfactory S/N ratio; the partial pressure of C_6H_5F in the photolysis region near the exit of the slit is likely greater than the observed average pressure in the chamber. C_6H_5F has an absorption cross section $\sim 1.9\times10^{-17}$ cm^2 at 193 nm.[26] An investigation of the dependence of signal intensity on the fluence of photolysis laser indicates that the signal intensity deviates from linearity when the laser fluence is greater than 50 mJ cm^{-2}. With a fluence greater than 65 mJ cm^{-2}, we recorded unresolved emission in the region 4000–10 000 cm^{-1} associated with multiphoton processes. Hence experiments performed only with a photolysis fluence<50 mJ cm^{-2} were used to determine the internal energy of HF. Although, based on time-resolved emission experiments, we are unable to exclude the slight possibility of production of HF from fragmentation of molecular ions that might be produced via a 1+1 REMPI process, we believe that such a contribution is negligible based on results from separate experiments using photofragmentation translational spectroscopy (to be published); observed translational energy of HF and C_6H_4 fit well with a single distribution and there is no evidence of production of HF from fragmentation of the parent ion.

A. Infrared emission of HF

Figure 1 shows partial emission spectra of HF, at a resolution of 2.0 cm^{-1}, recorded 0.1–0.6, 0.6–1.1, 1.1–1.6, and 1.6–2.1 μs after photolyses of C_6H_5F (0.013 Torr) and Ar (0.022 Torr). The small intensities in periods before 1.1 μs are partially due to the slow response of the detection system, the temporal evolution of the signal is described later. Assignments based on spectral parameters reported by Sengupta *et al.*[27] and Ram *et al.*[28] are shown as stick diagrams in

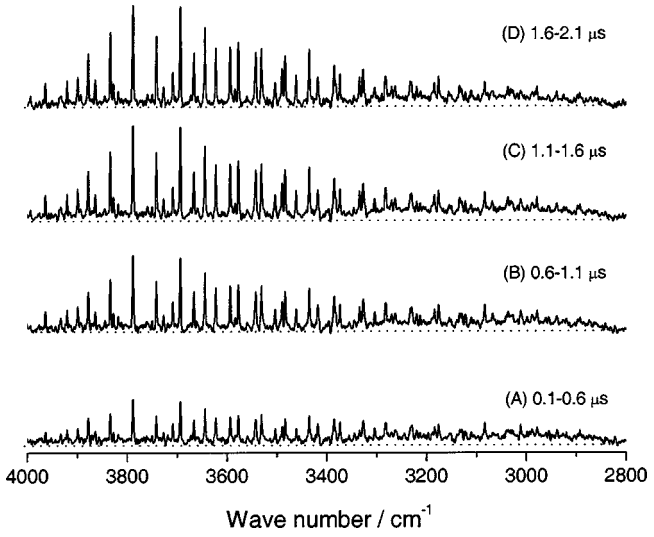

FIG. 1. Infrared emission spectra of HF in spectral region 2800–4000 cm^{-1} recorded at varied intervals after photolysis of C_6H_5F (0.013 Torr) in Ar (0.022 Torr) at 193 nm. (A) 0.1–0.6 μs; (B) 0.6–1.1 μs; (C) 1.1–1.6 μs; (D) 1.6–2.1 μs. Spectral resolution is 2.0 cm^{-1}; 27 laser pulses were averaged at each scan step of the interferometer.

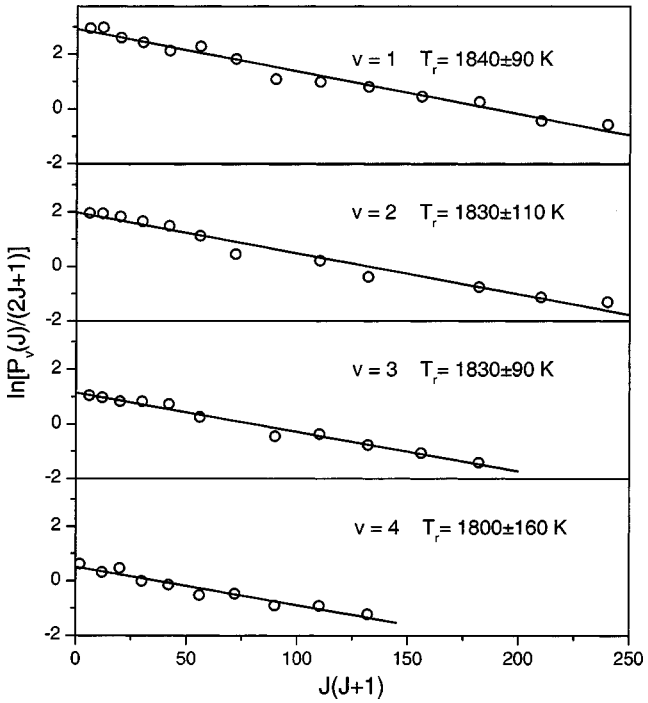

FIG. 3. Semilogarithmic plots of relative rotational populations of HF($v=1-4$) after photolysis of C_6H_5F (0.013 Torr) in Ar (0.022 Torr) at 193 nm. Solid lines represent least-squares fits.

Fig. 2; values of J' are indicated. The spectrum exhibits emission from HF with J' up to 15 and v up to 4. Each vibrational-rotational line in the P branch was normalized with the instrument response function and divided by its respective Einstein coefficient[29] to yield a relative population $P_v(J')$. Partially overlapped lines, such as $J'=4$, 6, 9, 11–13 of HF($v=1$), $J'=3$, 8, 9, 11–13 of HF($v=2$), $J'=2$, 7–9, 12 of HF($v=3$), and $J'=2$, 7, 9 of HF($v=4$), were deconvoluted to yield their intensities. Semilogarithmic plots of $P_v(J')/(2J'+1)$ versus $J'(J'+1)$ for HF($v=1-4$) produced from C_6H_5F are shown in Fig. 3. Fitted Boltzmann-type rotational distributions of HF, derived from the spectrum recorded in the range 0.1–1.1 μs, yield rotational temperatures of 1840±90, 1830±110, 1830±90, and 1800±160 K for $v=1-4$, respectively; unless specified, error limits listed in this paper represent one standard deviation in fitting. Similar procedures were carried out for spectra averaged over 1.1–2.1, 2.1–3.1, and 3.1–4.1 μs. With a short extrapolation, we estimate that the nascent rotational temperature to be 1930±20, 1920±20, 1920±40, and 1910±10 K for $v=1-4$, respectively; an average rotational temperature of 1920±140 K is thus derived; an estimated error is listed.

We assume a Boltzmann distribution and associate an interpolated population with overlapped lines. Relative populations obtained on counting levels up to observed J_{max} in

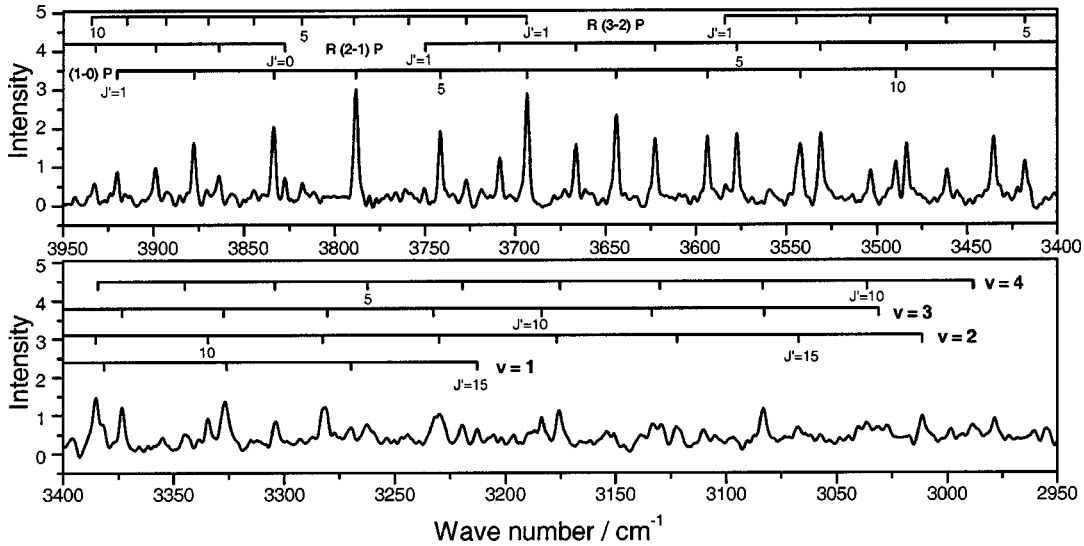

FIG. 2. Infrared emission spectra of HF in spectral region 2950–3950 cm^{-1} recorded 0.1–1.1 μs after photolysis of C_6H_5F (0.013 Torr) in Ar (0.022 Torr) at 193 nm. Spectral resolution is 2.0 cm^{-1}; 27 laser pulses were averaged at each scan step of the interferometer. Assignments are shown as stick diagrams.

TABLE I. Fitted rotational temperature, rotational energy, and vibrational population of HF(v) recorded 0.1–1.1 μs after photolysis of C_6H_5F at 193 nm.

v	T_{rot} (K)	$\Sigma_J P_v(J)$[a]	$E_r(v)$ (kJ mol^{-1})	Vibrational population[b]
0				0.562[c] (0.564)[d]
1	1840±90	1154[c] (1176)[d]	14.1[c] (15.2)[d]	0.262 (0.260)
2	1830±110	467(477)	13.9 (15.1)	0.106 (0.106)
3	1830±90	204(214)	12.5 (14.5)	0.046 (0.047)
4	1800±160	102(102)	10.4 (10.4)	0.024 (0.023)

[a]$P_v(J)$=(relative integrated emittance)/[(instrumental response factor)(Einstein coefficient)]; arbitrary unit.
[b]Normalized to $v=0-4$; populations of $v=0$ are estimated from extrapolation.
[c]Observed data. Only levels below observed J_{max} in each vibrational level are included; see text.
[d]Extrapolated data are listed parenthetically. All levels up to $E=17\,120$ cm^{-1} above the ground level are included; see text.

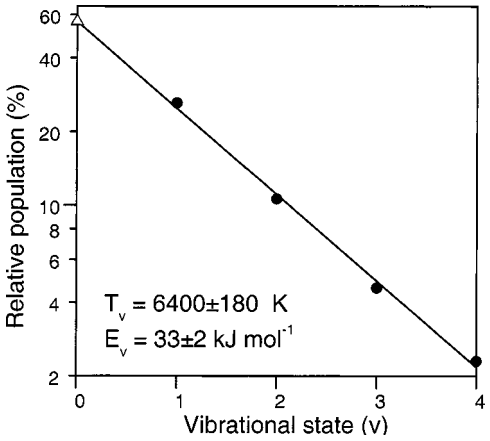

FIG. 4. Relative vibrational distributions of HF($v=0-4$) after photolysis of C_6H_5F (0.013 Torr) in Ar (0.022 Torr) at 193 nm. ●, from observed data; △, estimate by extrapolation.

each vibrational level (referred as ''observed data'' hereafter) are listed as $\Sigma_J P_v(J)$ in Table I. We normalized values of $\Sigma_J P_v(J)$ associated with each vibrational state to yield a relative vibrational population $(v=1):(v=2):(v=3):(v=4)=(60\pm7):(24\pm3):(10.5\pm0.9):(5.3\pm0.4)$, correspond to a vibrational temperature of 6400±180 K. Rotational energies for each vibrational level $E_r(v)$ obtained on summing a product of rotational level energy and normalized population for each rotational level, are also listed in Table I. An average rotational energy $E_r=13.7\pm1.6$ kJ mol^{-1} for HF($v=1-4$) observed 0.1–1.1 μs after photolysis is derived on summing a product of vibrational population and associated $E_r(v)$. After applying a correction factor 1920/1830=1.05 for rotational quenching, we derive a nascent rotational energy of 14.4±1.7 kJ mol^{-1} based on observed data.

The highest level of HF observed, $J'=11$ of $v=4$ has an energy 17 120 cm^{-1} above the ground vibrational level; this energy corresponds to $J_{max}(v)=26$, 22, and 17 for $v=1-3$, respectively. We assume a Boltzmann distribution and associate an extrapolated population with unobserved lines up to $J_{max}(v)$ for each vibrational level to derive a revised population distribution, referred to as ''extrapolated data'' hereafter; the relative rotational population $\Sigma_J P_v(J)$ and rotational energy $E_r(v)$ thus derived are listed in parentheses in Table I. An average rotational energy of 14.8±1.8 kJ mol^{-1} and a nascent rotational energy of $E_r=15.5\pm1.8$ kJ mol^{-1} estimated with a small correction for quenching are thus derived from extrapolated data. Taking this upper limit into account, *we report an average rotational energy of HF as* 15±3 kJ mol^{-1}.

Assuming a Boltzmann distribution, we estimate the population of $v=0$ relative to $v=1$ to be 2.14 and 2.17 for observed and extrapolated data, respectively. The vibrational distribution of HF normalized for $v=0-4$ is thus $(v=0):(v=1):(v=2):(v=3):(v=4)=56.2:26.2:10.6:4.6:2.4$ and 56.4:26.0:10.6:4.7:2.3 for observed and extrapolated data, respectively, as shown in Table I; the differences between observed and extrapolated data are negligible, so only the distribution derived from observed data is shown in Fig. 4. The average vibrational energies of HF derived from observed and extrapolated data are $E_v=32.7\pm2.4$ kJ mol^{-1}.

If the vibrational population has a smooth non-Boltzmann distribution, we may estimate a lower bound of the population of $v=0$ to be 1.3 times that of $v=1$. The average vibrational energy of $E_v=42$ kJ mol^{-1} thus derived might be taken as an upper limit. Taking this upper limit into account, *we report an average vibrational energy of HF as* 33±9/3 kJ mol^{-1}.

B. Unresolved emission in the 2800–3500 cm^{-1} region

A weak continuous emission in the range 2800–3400 cm^{-1} was present at an early stage ($t\leqslant5$ μs) after irradiation (Fig. 1) and diminished after $t\geqslant20$ μs; the lower bound of the spectrum might be limited by the transmission of the IR filter. With the present detectivity and resolution, we are unable to assign positively the carrier of this broad feature. A possible candidate is o-benzyne (C_6H_4). The C–H stretching modes of o-benzyne isolated in solid Ne absorb at 3049, 3071, 3086, and 3094 cm^{-1},[30] consistent with the observed region of emission. Emission of the internally excited parent C_6H_5F cannot, however, be positively excluded because C_6H_5F also absorbs in the region 3020–3130 cm^{-1}.

C. Temporal profiles of emission

The temporal evolution of emission of HF and the broad feature produced from photolysis of C_6H_5F (0.013 Torr) with Ar (0.022 Torr) at 193 nm is shown in Fig. 5. The total intensity for emission of the broad feature was derived by integration of the spectrum with features associated with HF subtracted at each time interval, whereas that of HF was derived by integration of lines with the broad feature removed. Emission of the broad feature reaches a maximum at ~1.4 μs, whereas that of HF reaches a maximum at ~2.9 μs; the variation is mainly due to a quenching rate for the broad feature (like o-benzyne) much greater than that for HF. We deconvoluted these profiles with the instrument response function and a mechanism consisting of formation and quenching in first order to derive rates of formation $k_f=(1.5\pm0.2)\times10^6$ and $(3.3\pm1.3)\times10^6$ s^{-1} and rates of quenching $k_q=(2.6\pm0.2)\times10^4$ and $(1.1\pm0.4)\times10^5$ s^{-1} for

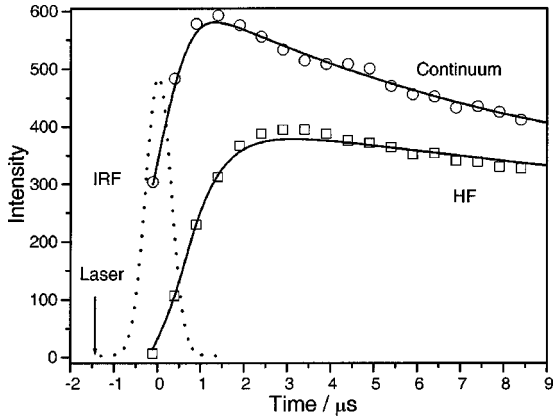

FIG. 5. Temporal profiles of HF (□) and the continuum in a region 2850–3450 cm^{-1} (○) after photolysis of C_6H_5F (0.013 Torr) in Ar (0.022 Torr) at 193 nm. IRF: instrument response function.

HF and the broad feature, respectively. Considering the error associated with the intensity of the broad feature, both HF and the broad feature have similar rates of production.

D. Calculations on transition states of C_6H_5F and branching ratios

We performed calculations to optimize structures of transition states for H-shift (TS2), three-center (TS3), and four-center (TS4) elimination channels of C_6H_5F with the B3LYP/6-311G(d,p) density-functional theory[31,32] using the GAUSSIAN 03 program.[33] Geometries of transition states TS2, TS3, and TS4 of C_6H_5F and displacement vectors corresponding to imaginary vibrational wave numbers predicted with the B3LYP method are shown in Fig. 6; available data derived previously[18] with B3LYP/6-31+G* are listed in parentheses for comparison. Predicted vibrational wave numbers for TS2, TS3, and TS4 of C_6H_5F are listed in Table II. Relative energies and barriers of the H-shift and both molecular elimination channels are shown in Fig. 7; estimates from a similar figure reported previously[18] using CCSD/6-311+G*//B3LYP/6-31+G* are listed in parentheses for comparison. Calculations using the B3LYP/6-311G(d,p) method yield barriers of 497 and 387 kJ mol^{-1} for three-center and four-center elimination channels, respectively, within 17 kJ mol^{-1} of those predicted using the CCSD method. The three-center elimination proceeds via a transition state TS2 with a barrier of 389 kJ mol^{-1} to form iso-C_6H_5F with energy nearly identical to TS2, followed by a further barrier of 108 kJ mol^{-1} to reach TS3.

We estimated rates of dissociation via these two channels on the ground electronic surface of C_6H_5F with a microcannonical transition-state theory. The Whitten-Rabinovitch equations[34] were used to calculate density of states. Using barriers of 497 and 387 kJ mol^{-1} and vibrational wave numbers listed in Table II, we calculated rates of dissociation for four-center and three-center elimination channels to be 8.7×10^5 and 89 s^{-1}, respectively; the latter was derived on assuming a steady-state of intermediate iso-C_6H_5F. Accordingly, production of HF via the three-center elimination path on the ground electronic surface is negligible.

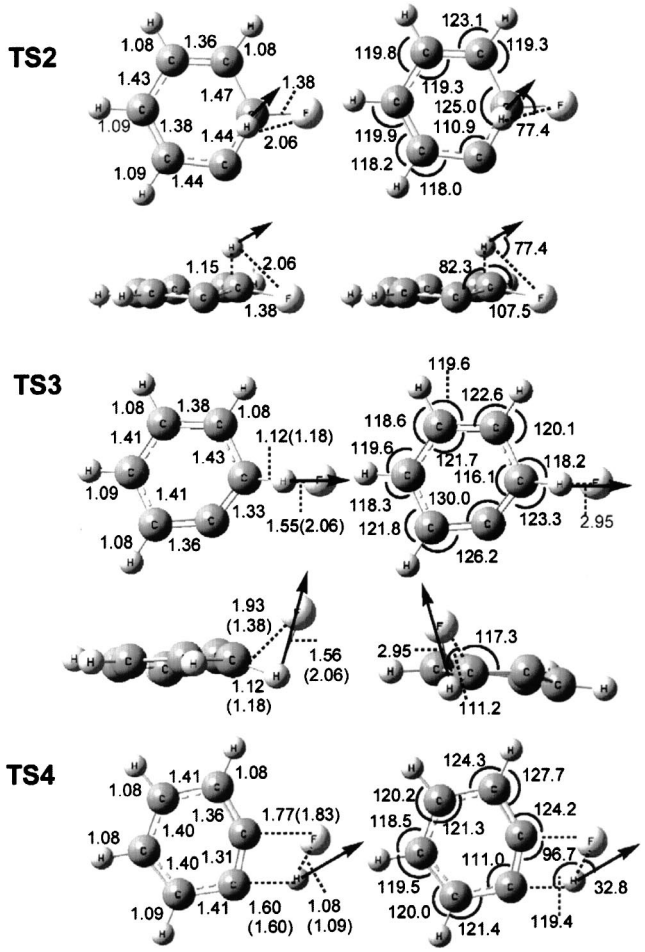

FIG. 6. Geometries of transition states for 1,2-H-shift (TS2), three-center elimination (TS3) and four-center elimination (TS4) of C_6H_5F predicted with the B3LYP/6-311G(d,p) method. TS2 and TS3 are nonplanar. Bond lengths (shown on the left) are in Å and bond angles (shown on the right) are in degrees (°). Results reported by Huang *et al.* using the B3LYP/6-31+G* method are shown in parentheses for comparison. Displacement vectors corresponding to imaginary wave numbers are shown with solid arrows.

IV. DISCUSSION

In experiments with a static cell, only C_2H_2 and 1,3-butadiyne (C_4H_2) were observed as end products. These products are likely produced from decomposition of C_6H_4 via secondary photolysis,[35]

$$C_6H_4 \rightarrow C_2H_2 + C_4H_2, \quad \Delta H = 251 \text{ kJ mol}^{-1}. \tag{4}$$

Enthalpies of formation for C_6H_4, C_2H_2, and C_4H_2 are 440 ±10, 226.7±0.8, and 464 kJ mol^{-1}, respectively.[36] The absence of HF might be due to reactions with the walls of the absorption cell or the multireflection optics in the cell. Observation of time-resolved emission of HF and possibly C_6H_4 with TR-FTS clearly demonstrates its superiority over conventional Fourier transform infrared (FTIR) spectrometer in investigating photodissociation processes.

Our previous investigation on photolysis of CH_2CHF (0.180 Torr) in Ar (0.270 Torr) showed that rotational quenching of HF(v,J) is small but nonnegligible. In this experiment we were able to use a total pressure as small as 0.035 Torr and employ a data acquisition window of 1.0 μs

TABLE II. Vibrational wave numbers (cm^{-1}) of transition states TS2, TS3, and TS4 of C_6H_5F predicted with the B3LYP/6-311G(d,p) method.

	Vibrational wave numbers (cm^{-1})									
TS2	3194	3176	3151	3128	2575	1637	1520	1440	1405	1306
	1220	1183	1167	1113	1101	1034	1006	991	924	892
	854	751	663	590	542	495	392	311	220	184*i*
TS3	3200	3188	3180	3160	2816	1667	1522	1463	1391	1336
	1245	1170	1130	1037	1020	976	956	924	901	843
	765	662	607	552	463	393	354	179	126	815*i*
TS4	3234	3188	3173	3155	1852	1741	1520	1479	1428	1321
	1258	1167	1116	1028	1010	988	933	925	899	854
	736	725	645	596	574	447	392	244	155	1166*i*

so that observed rotational quenching is nearly negligible; the correction to rotational temperature due to quenching is only ~5%. Vibrational quenching is negligible under our experimental conditions. It should be noted that the pressure in the photolysis region might be slightly greater than the pressure determined with the gauge because of the pressure gradient in the system.

According to a previous report[18] and RRKM (Rice-Ramsperger-Kassel-Marcus) calculations, HF is produced via the four-center elimination channel of C_6H_5F. The internal-energy distribution of HF observed in this work is also consistent with such a model, as discussed below.

A. Rotational energy of HF

Our previous experience[2,3] indicates that average rotational and vibrational energies of HF, produced via the four-center elimination channel, do not agree with predictions using phase-space theory[37–39] and separate statistical ensemble[40] models. A revised impulse model predicts satisfactorily the rotational energy of H*X* products. Assuming that the H atom receives most available energy, we distribute available energy between H and C atoms during bond breaking, followed by calculations of translational and rotational energy of HF according to classical mechanics. Instead of assuming that the H atom moves along the direction of the breaking bond as in the standard impulse model, we consider motions associated with the reaction coordinates described by displacement vectors associated with the imaginary vibrational frequency of transition state TS4 of C_6H_5F. The direction of the H atom is assumed to follow the displacement vector shown in Fig. 6. Rotational energies are predicted with this modified impulse model according to the equation

$$E_{\mathrm{rot}}=[m_{\mathrm{F}}m_{\mathrm{C}}/(m_{\mathrm{H}}+m_{\mathrm{F}})(m_{\mathrm{H}}+m_{\mathrm{C}})]E_{\mathrm{avail}}\sin^2\cdot\alpha, \qquad (5)$$

in which E_{avail} is the available energy (exit barrier) and α is the torque angle between the direction of motion of H and that of the H–F bond. With available energies of 56 and 166 kJ mol^{-1} and $\alpha=32.8°$ and 3.0° predicted for four-center and three-center elimination channels, respectively, rotational energies of 14.4 and 0.4 kJ mol^{-1} are predicted. The former is nearly identical to the experimental value of 15 ± 3 kJ mol^{-1}. Considering possible errors associated with the estimated exit barrier and the relatively simply impulse model, the agreement is satisfactory. The average rotational energy of 15 ± 3 kJ mol^{-1} for HF implies that a small fraction of total available energy is partitioned into HF, with $f_r\cong0.045\pm0.009$.

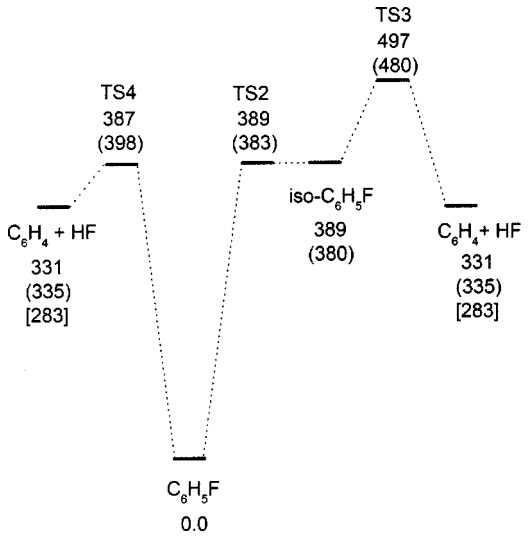

FIG. 7. Energies (in kJ mol^{-1}) of transition states (TS2, TS3, and TS4) and dissociation products relative to C_6H_5F. Energies are predicted with the B3LYP/6-311G(d,p) method; those from Ref. 18 using CCSD/6-311+G*//B3LYP/6-31+G* are shown in parentheses for comparison. The experimental value is in brackets.

B. Vibrational energy of HF

The average vibrational energy of $33\pm9/3$ kJ mol^{-1} for HF implies that a moderate fraction of available energy is partitioned into HF, with $f_v\cong0.10\pm0.03/0.01$. The partition of vibrational energy depends on the deviation of the distance between two bond-forming atoms from the equilibrium bond length. Predicted distances between H and F for TS3 and TS4 in dissociation of C_6H_5F are 1.56 and 1.08 Å, respectively. Because the equilibrium bond distance of HF is 0.9168 Å (Ref. 41), one would expect that the vibrational distribution of HF produced via the three-center elimination be highly inverted, in contrast to the vibrational distribution observed in this work. As a comparison, the distance between H and F in TS4 for four-center elimination of CH_2CHF is predicted to be 1.281 Å and the observed vibrational population of HF has a maximum near $v=1$ or 2.[5]

TABLE III. Comparison of total available energies, geometry of transition states, observed average internal energies, and predicted rotational energies of HF using a revised impulse model. All energies are in unit of kJ mol^{-1}. E_{ava}, available energy; E_{exit}, exit barrier; α, torque angle of TS4; E_v, vibrational energy; E_r, rotational energy.

Species	E_{ava}	E_{exit}	R_{HF} (TS4) (Å)	α (deg)	E_v (expt.)	E_r (expt.)	E_r (impulse)[a]	Reference
CH_2CHF	528	219	1.28	8.2	83±9	2.5±1.5[b]	3.9	3
CF_2CHCl	458	199	1.18	17.5	46±6	20±4	15.8	5
C_6H_5F	284	56	1.08	32.8	33±9/3	15±3	15.4	This work

[a]Assuming that the motion of H atom is along the displacement vector corresponding to the imaginary mode of the transition state; see text.
[b]Recent trajectory calculations (Ref. 43) indicate that the four-center elimination channel produces high-J components; see text.

With a distance of 1.08 Å for TS4, one would expect the $v=0$ or 1 level of HF product to have the greatest population. Hence, the observed vibrational distribution of HF fits satisfactorily with the four-center elimination mechanism.

C. Energy balance

In previous work using multimass imaging detection, the distribution of translational energy release of reaction (2) upon photolysis at 193 nm is reported to show a maximum at 155 kJ mol^{-1} and a decreasing population extending to the maximum available energy ~336 kJ mol^{-1}.[18] We estimated an average translational energy of ~146 kJ mol^{-1} from their distribution plot; this value implies that the fraction of energy partitioned into translation is $f_t \cong 0.43$.

With an available energy of 336 kJ mol^{-1} and an observed average translational release of 146 kJ mol^{-1}, 190 kJ mol^{-1} is distributed between internal energies of HF and C_6H_4. Our observation of ~48 kJ mol^{-1} in internal energy of HF implies that C_6H_4 has an average internal energy of 142 kJ mol^{-1}. If available energy above the barrier were distributed statistically, one would expect that most energy would be partitioned to C_6H_4 because of its high degree of freedom relative to the other fragment HF. Our observation clearly indicates that the statistical model fails in this case. The dissociation energy of C_6H_4 to form C_2H_2 and C_4H_4,

$$C_6H_4 \rightarrow C_2H_2 + C_4H_2, \quad (4)$$

is ~251 kJ mol^{-1}; hence most C_6H_4 undergoes no further dissociation unless it absorbs a second photon.

We noticed that the previously reported translational energy of 146 kJ mol^{-1} for the C_6H_4+HF channel, determined from the velocity distribution of C_6H_4, is atypically large; the exit barriers predicted with B3LYP/6-311G(d,p) in this work and CCSD/6-311+G*//B3LYP/6-31+G* are only 56 and 63 kJ mol^{-1}, respectively. The reason for this discrepancy is unclear. Possibilities include interference from multiphoton processes, decomposition of some C_6H_4 with a large internal energy (hence a small kinetic energy), significant access of regions well above TS4, and an unexpectedly large error in calculations of the exit barrier for the four-center elimination channel. Further study using a molecular beam system utilizing synchrotron radiation for ionization is scheduled. Although the exit barrier of the three-center elimination, 166 kJ mol^{-1}, fits satisfactorily with the observed average translational energy, this possibility is excluded based on the internal-energy distribution of HF observed in this work and RRKM calculations.

D. Rate of production and quenching

Huang *et al.* reported a rate of $(1.4\pm0.8)\times10^6$ s^{-1} for production of C_6H_4.[18] After deconvolution of temporal profiles of HF with the instrument response function, we obtained a rate of formation of $(1.5\pm0.2)\times10^6$ s^{-1} for HF, nearly identical to their results.

According to Huang *et al.*,[18] absorption of 193 nm photons corresponds to excitation of C_6H_5F to the S_3 state, which internally converts to the ground S_0 state, followed by four-center HF-elimination (major channel) and C–H fission (minor channel).[18] They performed RRKM calculations and obtained rates of formation of HF via three-center and four-center elimination channels to be 2.2×10^3 and 1.1×10^6 s^{-1}, respectively; a steady-state approximation was employed for the intermediate formed after a 1,2-H shift and before the three-center elimination. The rate of formation of HF based on energies predicted with B3LYP/6-311G(d,p) for four-center elimination is 8.7×10^5 s^{-1}, consistent with experimental and previous calculation results.

The observed rate of quenching for HF, $(2.6\pm0.2)\times10^4$ s^{-1}, at $[C_6H_5F]=4.2\times10^{14}$ molecule cm^{-3} implies an apparent bimolecular rate coefficient for vibrational quenching $k_q^{II}=(6.3\pm0.5)\times10^{-11}$ cm^3 molecule^{-1} s^{-1} by C_6H_5F; vibrational quenching of HF by Ar is much smaller than that by C_6H_5F.[42] This rate represents mainly quenching from the $v=1$ state of HF. We did not study detailed rates of quenching for each individual vibrational state. A rate of quenching for the broad feature greater than that of HF is conceivable, as the possible carrier C_6H_4 for the broad feature is more complex than HF and is similar to C_6H_5F; hence quenching of C_6H_4 is expected to proceed more readily.

E. Comparison with photolysis of other fluoro-compounds

The observed rotational energies of HF from four-center elimination channels of C_6H_5F and CF_2CHCl are compared with those predicted according to the modified impulse model in Table III. Although the total available energies and the exit barriers for these two systems vary substantially,

observed rotational energies of HF agree satisfactorily with those predicted with the modified impulse model. Rotational excitation of HF produced from four-center elimination of CH_2CHF is not compared because recent trajectory calculations indicate that the four-center elimination produces more rotationally excited HF and the low-J component of HF observed previously[3] might be due to quenching.[43] Further experiments are needed to clarify this discrepancy. That HF produced from CF_2CHCl and C_6H_5F, both via four-center elimination, has greater rotational energy is consistent with a significant torque angle in their TS4. The torque angle of 32.8° for TS4 of C_6H_5F is nearly twice that of CF_2CHCl, but its exit barrier is only $56/199=0.28$ that for CF_2CHCl; the resultant rotational energies of HF in these two systems are consequently similar.

Likewise, average vibrational energies of HF via four-center elimination of these molecules are compared in Table III. HF produced via four-center elimination of CH_2CHF has more vibrational energy (83 ± 9 kJ mol^{-1}) than that (48 ± 6 kJ mol^{-1}) from CF_2CHCl because predicted bond distances of TS4 are 1.28 and 1.18 Å, respectively. Calculated wave functions also indicate that the H-F bond is ''formed'' in TS4 of CF_2CHCl and C_6H_5F, whereas the H-F bond in TS4 of CH_2CHF are not yet formed. The vibrational energy of HF, $33\pm9/3$ kJ mol^{-1}, from photolysis of C_6H_5F is the smallest, consistent with the shortest H-F distance 1.08 Å calculated for TS4; it is nearest the equilibrium distance of HF.

V. CONCLUSION

Rotationally resolved emission of HF up to $v=4$ is observed after photolysis of C_6H_5F at 193 nm; HF is likely produced from the four-center elimination channel on the ground electronic surface. The average rotational energy of 15 ± 3 kJ mol^{-1} and vibrational energy of $33\pm9/3$ kJ mol^{-1} for HF implies that a moderate fraction of available energy is partitioned into the internal energy of HF, with $f_v\cong0.10\pm0.03/0.01$ and $f_r\cong0.045\pm0.009$. A modified impulse model considering displacement vectors of transition states during bond breaking predicts the average rotational energy of HF satisfactorily for four-center elimination channels of CF_2CHCl and C_6H_5F. Partition of vibrational energy into HF upon photolysis is also consistent with distances of H-F predicted for transition states of four-center elimination for these systems.

ACKNOWLEDGMENTS

The authors thank the National Science Council of Taiwan (Grant No. NSC92-2113-M-007-034) and the Ministry of Education of Taiwan (Program for Promoting Academic Excellence of Universities, Grant No. 89-FA-04-AA) for support and the National Center for High Performance Computing for computer time.

[1] Y.-P. Lee, Annu. Rev. Phys. Chem. **54**, 215 (2003).
[2] S.-R. Lin, S.-C. Lin, Y.-C. Lee, Y.-C. Chou, I-C. Chen, and Y.-P. Lee, J. Chem. Phys. **114**, 160 (2001).
[3] S.-R. Lin, S.-C. Lin, Y.-C. Lee, Y.-C. Chou, I-C. Chen, and Y.-P. Lee, J. Chem. Phys. **114**, 7396 (2001).
[4] D. A. Blank, W. Sun, A. G. Suits, Y. T. Lee, S. W. North, and G. E. Hall, J. Chem. Phys. **108**, 5414 (1998).
[5] C.-Y. Wu, C.-Y. Chung, Y.-C. Lee, and Y.-P. Lee, J. Chem. Phys. **117**, 9785 (2002).
[6] C.-Y. Wu, Y.-P. Lee, J. F. Ogilvie, and N. S. Wang, J. Phys. Chem. A **107**, 2389 (2003).
[7] C.-Y. Wu, Y.-P. Lee, and N. S. Wang, J. Chem. Phys. **120**, 6957 (2004).
[8] A. M. Mebel, M. C. Lin, D. Chakraborty, J. Park, S. H. Lin, and Y. T. Lee, J. Chem. Phys. **114**, 8421 (2001), and references therein.
[9] S.-T. Tsai, C.-L. Huang, Y. T. Lee, and C.-K. Ni, J. Chem. Phys. **115**, 2449 (2001).
[10] C.-K. Lin, C.-L. Huang, J.-C. Jiang, H. H. Chang, Y. T. Lee, S. H. Lin, and C.-K. Ni, J. Am. Chem. Soc. **124**, 4068 (2002).
[11] A. Freeman, S. C. Yang, M. Kawasaki, and R. Bersohn, J. Chem. Phys. **72**, 1028 (1980).
[12] T. Ichimura, Y. Mori, H. Shinohara, and N. Nishi, Chem. Phys. **189**, 117 (1994).
[13] T. Ichimura, Y. Mori, H. Shinohara, and N. Nishi, Chem. Phys. Lett. **122**, 55 (1985).
[14] K.-L. Han, G.-Z. He, and N.-Q. Lou, Chem. Phys. Lett. **203**, 509 (1993).
[15] G.-J. Wang, R.-S. Zhu, H. Zhang, K.-L. Han, G.-Z. He, and N.-Q. Lou, Chem. Phys. Lett. **288**, 429 (1998).
[16] H. Zhang, R.-S. Zhu, G.-J. Wang, K.-L. Han, G.-Z. He, and N.-Q. Lou, J. Chem. Phys. **110**, 2922 (1999).
[17] M. Dzvonik, S. Yang, and R. Bersohn, J. Chem. Phys. **61**, 4408 (1974).
[18] C.-L. Huang, J.-C. Jiang, A. M. Mebel, Y. T. Lee, and C.-K. Ni, J. Am. Chem. Soc. **125**, 9814 (2003).
[19] *CRC Handbook of Chemistry and Physics*, 78th ed., edited by D. R. Lide (RC, New York, 1997).
[20] M. W. Chase, Jr., J. Phys. Chem. Ref. Data Monogr. **9**, (1998).
[21] J. M. Riveros, S. Ingeman, and N. M. M. Nibbering, J. Am. Chem. Soc. **113**, 1053 (1991).
[22] P. G. Wenthold and R. R. Squires, J. Am. Chem. Soc. **113**, 7414 (1991); **116**, 6401 (1994).
[23] W. Tsang, in *Energetics of Organic Free Radicals*, edited by J. A. Martinho Simoes, A. Greenberg, and J. F. Liebman (Blackie Academic and Professional, London, 1996), Vol 4, pp. 22–58.
[24] P.-S. Yeh, G.-H. Leu, Y.-P. Lee, and I.-C. Chen, J. Chem. Phys. **103**, 4879 (1995).
[25] S.-R. Lin and Y.-P. Lee, J. Chem. Phys. **111**, 9233 (1999).
[26] K. Bowden and E. A. Braude, J. Chem. Soc. 1068 (1952).
[27] U. K. Sengupta, P. K. Das, and K. N. Rao, J. Mol. Spectrosc. **74**, 322 (1979).
[28] R. S. Ram, Z. Morbi, B. Guo, K.-Q. Zhang, P. F. Bernath, J. V. Auwera, J. W. C. Johns, and S. P. Davis, Astrophys. J., Suppl. Ser. **103**, 247 (1996).
[29] E. Arunan, D. W. Setser, and J. F. Ogilvie, J. Chem. Phys. **97**, 1734 (1992).
[30] J. G. Radziszewski, B. A. Hess, Jr., and R. Zahradnik, J. Am. Chem. Soc. **114**, 52 (1992).
[31] A. D. Becke, J. Chem. Phys. **98**, 5648 (1993).
[32] C. Lee, W. Yang, and R. G. Parr, Phys. Rev. B **37**, 785 (1988).
[33] M. J. Frisch, G. W. Trucks, H. B. Schlegel *et al.*, GAUSSIAN03, *Revision A.1* (Gaussian Inc., Pittsburgh, PA, 2003).
[34] K. A. Holbrook, M. J. Pilling, and S. H. Robertson, *Unimolecular Reactions*, 2nd ed. (Chichester, New York, 1996).
[35] W.-Q. Deng, K.-L. Han, J.-P. Zhan, and G.-Z. He, Chem. Phys. Lett. **288**, 33 (1998).
[36] H. Y. Afeefy, J. F. Liebman, and S. E. Stein, in *Neutral Thermochemical Data*, NIST Chemistry WebBook, NIST Standard Reference Database Number 69, edited by P. J. Linstrom and W. G. Mallard (National Institute of Standards and Technology, Gaithersburg, MD, 2003), p. 20899; http://webbook.nist.gov
[37] P. Pechukas and J. C. Light, J. Chem. Phys. **42**, 3281 (1965).
[38] C. E. Klots, J. Phys. Chem. **75**, 1526 (1971).
[39] M. Hunter, S. A. Reid, D. C. Robie, and H. Reisler, J. Chem. Phys. **99**, 1093 (1993).
[40] C. Wittig, I. Nadler, H. Reisler, M. Noble, J. Catanzarite, and G. Radhakrishnan, J. Chem. Phys. **83**, 5581 (1985).
[41] K. P. Huber and G. Herzberg, *Constants of Diatomic Molecules* (Van Nostrand, Princeton, 1979).
[42] S. R. Leone, J. Phys. Chem. Ref. Data **11**, 953 (1982), and references therein.
[43] E. Martínez-Núñez and S. A. Vázqucz, J. Chem. Phys. **121**, 5179 (2004).